

# A study on the variations of water temperature and sonar performance using the empirical orthogonal function scheme in the East Sea of Korea

## 동해에서 경험직교함수 기법을 이용한 수온과 소나성능 변화 연구

Young-Nam Na,<sup>1†</sup> Changbong Cho,<sup>1</sup> Su-Uk Son,<sup>1</sup> and Jooyoung Hahn<sup>1</sup>

(나영남,<sup>1†</sup> 조창봉,<sup>1</sup> 손수욱,<sup>1</sup> 한주영<sup>1</sup>)

<sup>1</sup>Agency for Defense Development (Maritime Technology R & D Institute)

(Received August 31, 2023; revised October 23, 2023; accepted November 13, 2023)

**ABSTRACT:** For measuring the performance of passive sonars, we usually consider the maximum Detection Range (DR) under the environment and system parameters in operation. In shallow water, where sound waves inevitably interacts with sea surface or bottom, detection generally maintains up to the maximum range. In deep water, however, sound waves may not interact with sea surface or/and bottom, and thus there may exist shadow zones where sound waves can hardly reach. In this situation, DR alone may not completely define the performance of each sonar. For complete description of sonar performance, we employ the concept ‘Robustness Of Detection (ROD)’. In the coastal region of the East Sea, the spatial variations of water masses have close relations with DR and ROD, where the two parameters show reverse spatial variations in general. The spatial and temporal analysis of the temperature by employing the Empirical Orthogonal Function (EOF) shows that the 1-st mode represents typical pattern of seasonal variation and the 2-nd mode represents strength variations of mixed layers and currents. The two modes are estimated to explain about 92 % of the variations. Assuming two types of targets located at the depths of 5 m (shallow) and 100 m (deep), the passive sonar performance (DR) gives high negative correlations (about -0.9) with the first two modes. Most of temporal variations of temperature occur from the surface up to 200 m in the water column so that when we assume a target at 100 m, we can expect detection performance of little seasonal variations with passive sonars below 100 m.

**Keywords:** Detection range, Robustness of detection, Passive sonar performance, Water mass, Mode and sonar performance

**PACS numbers:** 43.30.Cq, 43.30.Wi

**초 록:** 수동형 소나의 성능을 측정하기 위해 주어진 환경과 시스템 변수 하에서 보통 최대 탐지거리를 고려한다. 음파가 해표면 또는 해저면과 필연적으로 접촉하는 천해에서는 표적탐지가 최대 탐지거리까지 유지되는 게 일반적이다. 그러나 심해에서는 음파가 해표면 또는 해저면과 접촉하지 않을 수도 있으며, 이 경우 음파가 도달하지 않는 음영구역이 존재할 수도 있다. 이 경우 최대 탐지거리만으로 각 소나의 탐지성능을 완전하게 기술하기 어려울 수 있다. 보다 완전한 탐지성능 기술을 위해 ‘탐지견고성(Robustness Of Detection, ROD)’ 개념을 도입하고자 한다. 동해 연안에서 수괴의 공간적 분포와 최대 탐지거리 및 탐지견고성은 밀접한 관계가 있으며, 최대 탐지거리와 탐지견고성은 서로 반대의 공간적 변동을 보인다. 경험직교함수(Empirical Orthogonal Function, EOF)를 도입하여 수온의 시공간적 분포를 분석한 결과 첫 번째 모드는 전형적인 계절 변화를 보이고, 두 번째 모드는 혼합층 등의 세기 변화를 반영하는 것으로 추정된다. 이 두 모드가 전체 변화의 약 92 %를 설명한다. 수심 5 m와 100 m 표적을 가정하여 수동형 소나의 최대 탐지거리와 두 모드의 계절 변화의 상관관계를 분석하면 첫 두 모드와 높은 음의 상관계수(약 -0.9)를 보인다. 수온의 계절적 변화는 표층~수심 200 m에서 발생하며, 이에 따라 수심 100 m에 표적이 존재한다고 가정하여 수동소나를 수심 100 m 이상에서 운용할 경우 계절변화가 미미한 탐지성능을 기대할 수 있다.

**핵심용어:** 탐지거리, 탐지견고성, 수동소나성능, 수괴, 모드와 소나성능

†Corresponding author: Young-Nam Na (ynna@add.re.kr)

Agency for Defense Development (Maritime Technology R & D Institute), P. O. Box 18, Changwon, Gyeongnam 51678, Republic of Korea

(Tel: 82-55-540-6322, Fax: 82-55-542-3737)

“이 논문은 2023년도 한국음향학회 춘계학술대회에서 발표한 논문임”



Copyright©2024 The Acoustical Society of Korea. This is an Open Access article distributed under the terms of the Creative Commons Attribution Non-Commercial License which permits unrestricted non-commercial use, distribution, and reproduction in any medium, provided the original work is properly cited.

## I. Introduction

The East Sea of Korea is known to have many water masses which are identified by their physio-chemical properties such as temperature, salinity and dissolved oxygen.<sup>[1]</sup>

Concerning the waves propagation related to ocean environments, there were some studies whose interests include polar front,<sup>[2]</sup> mesoscale warm eddy,<sup>[3,4]</sup> and bathymetry.<sup>[5]</sup> There were also studies focused on sonar performances for decision aids of naval operations.<sup>[6,7]</sup> All of these works, however, deal with the effects of single environmental factor on waves propagation or sonar performance in specific time and space.

This paper tries to examine the relations between water masses and sonar performances in the coastal region of Korea. The relations include the variations in temporal and spatial domains in the study area. The behaviors of acoustic waves in water are determined by sound speeds. Since, temperature is generally dominant factor determining sound speed, we consider temperature as key parameter for water mass analysis.

For measuring the performance of passive sonars, we usually consider maximum Detection Range (DR) under the environment and system parameters in operation. In shallow water, where sound waves inevitably interact with sea surface or bottom, detection generally maintains up to the maximum range. In deep water, however, sound waves may not interact with sea surface or/and bottom, and thus there may exist shadow zones where sound waves can hardly reach. In this situation, DR alone may not provide complete definition the performance of each sonar. For the sonar performances in deep water, in addition to the existing DR, we adopt another concept Robustness Of Detection (ROD). For the analysis of temporal and spatial variations of temperature, we use the database, Korean Ocean Temperature Model (KOTM) 3.0,<sup>[8,9]</sup> which has 5-days means at each depth and every 5'x5' grid point around Korean peninsula. We employ the Empirical Orthogonal Function (EOF) scheme to get the temperature

variations.

Assuming two types of underwater targets at 5 m and 100 m, we examine the relations among the three factors : temperature, DR, and ROD. As an example of (passive) sonar operation related to seasonal variations of temperature, we give the comparisons of detection performance in February and August assuming a target at 100 m.

## II. Analysis methods

### 2.1 Robustness of Detection (ROD)

In measuring sonar performances, we can employ some sorts of concepts. The popular ones are 'effective range', 'near-continuous range' and 'maximum Detection Range (DR)'.<sup>[8]</sup> Among these, the concept 'DR' is generally considered to measure the long range detection including shadow and convergence zones.

We can calculate the DR at each grid point as following.

$$DR = \sum_{i=1}^N D_i / N, \quad (1)$$

Here,  $D_i$  and  $N$  are the maximum DR at the  $i$ -th bearing and its number equally divided in 360°. However, it may not provide complete definition to measure the performance of a sonar, particularly in deep water. It may not guarantee consistent detection when there exist shadow zones in horizontal and vertical directions.

For complete description of sonar performance, we employ another definition 'ROD' as following.<sup>[8]</sup>

$$ROD = \frac{D_B - D_A}{D_B} \times 100 (\%). \quad (2)$$

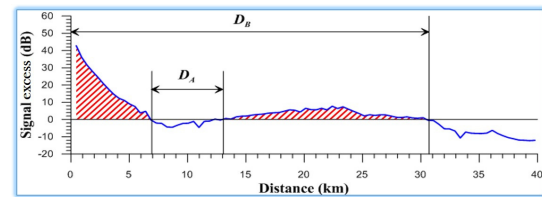


Fig. 1. (Color available online) Shadow range ( $D_A$ ) and maximum detection range ( $D_B$ ).

Here,  $D_A$  and  $D_B$  denote shadow range and maximum DR, respectively. Fig. 1 shows the definitions.

## 2.2 Empirical Orthogonal Function (EOF)

In waters of less than 500 m, sound speed is mainly determined by temperature. Temperature variation may be analyzed using the EOF method. Spatio-temporal variations of temperature ( $T$ ) may be decomposed into modal structure ( $A_n$ ) and corresponding time coefficients ( $B_n$ ) for each mode  $n$  as following.<sup>[9]</sup>

$$T(x, y, z, t) = \sum_n A_n(x, y, z) B_n(t). \quad (3)$$

Solving the eigen-value problems, we can get the reduced form of spatial variations,<sup>[9]</sup>

$$\frac{1}{N} (T T^t) \vec{e}_i = \lambda_i \vec{e}_i, \quad (4),$$

where  $T$ ,  $\vec{e}_i$ ,  $\lambda_i$ ,  $N$  denote the temperature covariance matrix, eigen-vector, eigen-value and number of spatial points, respectively.  $T^t$  represents the transpose of matrix  $T$ . The modal structure  $A_n$  is normalized to magnitude of standard deviation of  $B_n$  to have a physical unit  $^{\circ}\text{C}$ , while  $B_n$  has not any physical unit. The fraction of  $i$ -th mode contribution to the total  $N$  modes of variation may be expressed as  $\lambda_i / \sum_{i=1}^N (\lambda_i)$ .

## 2.3 Temperatures/sound speeds

We use the temperature database, KOTM 3.0,<sup>[8]</sup> which is the establishment of an average climatological marine environment data set for building up a sound exploration environment by re-analyzing the high resolution data around the Korean peninsula. The re-analyzed database was constructed by ensemble analysis over ocean numerical model results by verifying with observations from 1993 to 2018.<sup>[9]</sup> The data set includes 5-days mean temperature, salinity and sound speed at each grid point of horizontal resolution  $1/12^{\circ} \times 1/12^{\circ}$ . At each grid, the data set gives

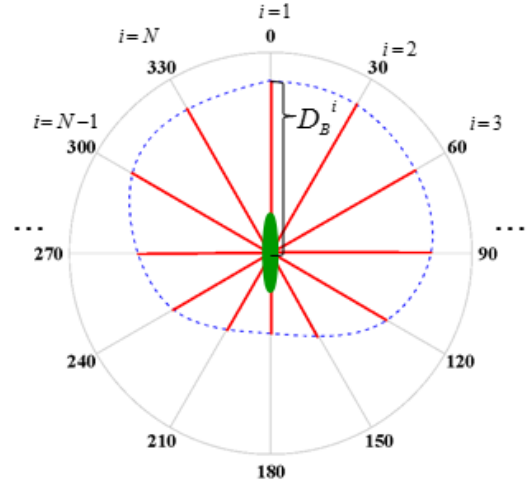


fig. 2. (color available online) schematic diagram showing the maximum detection ranges ( $D_B$ ) of 12 bearing angles at each point and depth.

non-linear depth resolution from the surface to the maximum depth of 6,000 m. From the data set, we select temperature or sound speed of every 10 m depth from the surface to 500 m in the study area.

The study area, about 200 km (longitude)  $\times$  200 km (latitude), has 82 grid points. At each point and every 10 m depth, we define the DR or ROD of each bearing, whose interval is  $30^{\circ}$ . Fig. 2 shows the 12 equal bearings of  $30^{\circ}$  interval with its DR ( $D_B$ ). By averaging DRs or RODs over all bearings, we get the mean DR or ROD at each depth and point. Again, we normalize the mean DR to the maximum in all depths and points to get relative values in ratio.

## 2.4 Propagation model

We use an acoustic model based on the Gaussian beam tracing scheme<sup>[10]</sup> to get acoustic fields (propagation loss) for 12 bearings at each depth and grid point. Since we consider the performance of passive sonars of mid-frequency, each depth of a grid point is the source position. From the propagation loss, we can compute DR or ROD by employing proper environment or system parameters such as noise level, directivity index, detection threshold etc. Since we are to examine the relations between water masses and sonar performances, we select the same parameters except propagation loss. In calculating

propagation loss, we assume the same geoacoustic characteristics in the sediment layer at all grid points so that the propagation loss only reflects temperature or sound speed effect.

### III. Analysis Results

#### 3.1 Water mass vs. Sonar performance

We give an example showing the relation between the DR and ROD, as defined in the section 2.1. Fig. 3 presents horizontal distributions of water depth (a), temperature (b), DR (c), and ROD (d). The temperature distribution comes from the data set re-analyzed at October 28, 2008. Depth distribution [Fig. 3(a)] shows that most of the area is actually deeper than 1,000 m, specially in northwestern and southeastern regions, except the coastal regions. The marked area in the southern part is regarded as continental shelf. Temperature distribution at 50 m [Fig. 3(b)] shows that cold water North Korean Cold Currents (NKCC) flows along the coast while warm water East Korean Warm Currents (EKWC) exist off the coast as shown in black and red arrows, respectively. The warm water is considered as related with meso-scale phenomena such as

eddies and thermal fronts. Using the water depth and temperature data set as environmental input to the acoustic model, we calculate the DR and ROD assuming the source and receiver depth to be 50 m. Fig. 3(c) gives an example of DR in ratio relative to the maximum value calculated for all grid points and vertical depths considered. From the distribution, we can see that the ratios are relatively high in the northwestern and southeastern regions where depths are more than 1,500 m as in Fig. 3(a). On the other hand, in the regions of shallower depths (marked in broken line) and northern warm water [red arrow in Fig. 3(b)], we can see very low ratios. These low DRs may be caused by frequent bottom interactions of acoustic waves in the warm water region, leading large propagation loss. Another sonar performance, ROD [Fig. 3(d)] shows reverse patterns in general with that of DR. That is, the ROD gives low values in the deep regions in the northwest and southeast while high values in the regions of shallower depths (marked in broken line) and northern warm water [red arrow in Fig. 3(b)].

As an another example showing the relation between water mass and detection performance, we present the temperature variations of 5 m and 100 m from the data set re-analyzed at February 21, 2007, and the corresponding DRs at source/receiver combinations of 100/5 m and 100/100 m, respectively. The surface temperatures [Fig. 4(a)] shows that the cold waters appear along the coast from northwestern region while the warm waters do in most of the area. At 100 m depth distribution [Fig. 4(b)], we can see that the cold waters develop much farther to the south along the coast and to the east, occupying most of the area.

The corresponding DRs [Fig. 4(c), (d)] gives clear relations with the temperatures. That is, the DRs show high values in the area of cold waters but low values in the area of warm waters. We try analyses over other horizontal distributions of temperature, DR and ROD and find that the two facts are still valid; 1) Temperature (water mass) variations are closely related to DR and ROD, 2) DR and ROD have general reverse patterns.

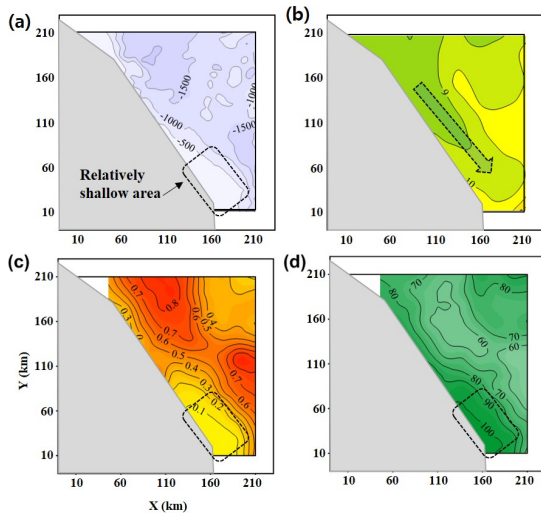


Fig. 3. Horizontal variations of environment and sonar performance. (a) water depth, (b) temperature (50 m, October 28, 2008), (c) DR (SD/RD = 50/50 m), (d) ROD (SD/RD = 50/50 m).

Using Eq. (3) in section 2.2, we can calculate the spatial amplitudes  $\{A_n(x,y,z)\}$  and principal components  $\{B_n(t)\}$  for each mode  $n$  at each point. In order to examine the seasonal variation of each mode, we find the mean amplitude and mean principal component by averaging over the coordinate  $(x,y,z)$  at each time. Concerning the sonar performance, we assume two kinds of source located near the surface (5 m) and deep (100 m) while the two kinds of receivers to be at 100 m. The two receivers have different specifications so that they show different performance for the same environment and targets. Using

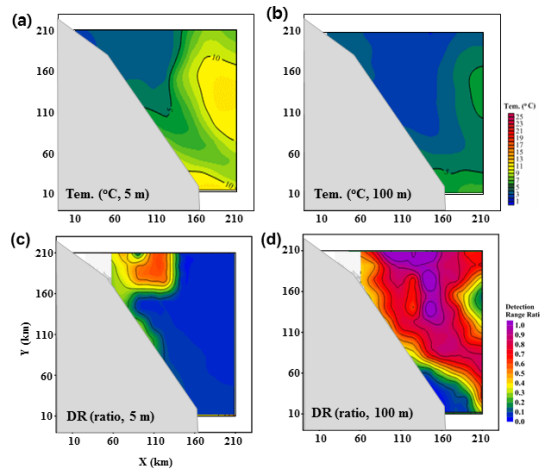


Fig. 4. Horizontal variations of environment and sonar performance. (a) temperature (0 m, February 21, 2007), (b) temperature (100 m, February 21, 2007), (c) DR (SD/RD = 100/5 m), (d) DR (SD/RD = 100/100 m).

these source and receiver configurations, we find the mean DR at each grid point as mentioned in section 2.3, and then find the total mean DR by averaging over all points at each time.

Fig. 5 shows the seasonal variations of modal amplitude multiplied by principal component (up) and sonar performances (down) where time step is 10 days. From the first two modes of temperature variations, we can see that mode1 ('+' symbols) follows typical patterns of seasonal variation while mode 2 ('◆' symbols) does not. We give the y-axis as reversed for the comparisons with the variations of sonar performance. Concerning the contribution to the total spatial variation in the study area, we estimate that the 1-st EOF mode accounts for 78 % and the 2-nd mode does 14 %.<sup>[13]</sup> Mode 1 is regarded as representing typical seasonal variation of water masses both in surface (warm) and deep (cold) layers, while mode 2 representing the strength variation of surface mixed layer and the East Korean Warm Currents.<sup>[13]</sup>

The sonar performance (Fig. 5, down), DR, which is averaged over all depths and grid points in the study area, gives seasonal variations for the four cases, two targets (located at 5 m and 100 m) and two receivers (different sonar types, located at 100 m). Comparing with the modal variations (Fig. 5, up), we can note that the DR for the surface target (source depth 5 m, '●' and '■' symbols) shows typical seasonal patterns and resembles the

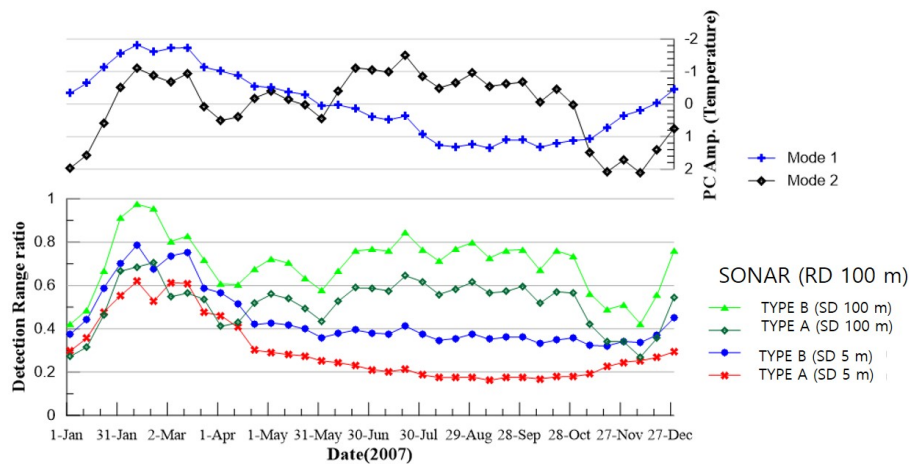


Fig. 5. Seasonal variations of the first two modes (°C, up) and DR (ratio, down) (RD = 5/100 m, SD = 100 m).



variations of mode 1 ('+' symbols). The correlation coefficients between the variations of mode 1 and DR give very high negative values,  $-0.87$  (Type A) and  $-0.94$  (Type B). On the other side, we can see that the DR variation for the deep target (source depth 100 m, '□' and '▲' symbols) shows similar patterns to the variations of mode 2 ('◆' symbols). The correlation coefficients between the variations of mode 2 and DR also give very high negative values,  $-0.89$  (Type A) and  $-0.93$  (Type B).

### 3.2 Water mass vs. Sonar operation

In this section, we give an example of sonar operation related to the water mass variation. In order to estimate the vertical limit of seasonal temperature variations, we review the horizontal distributions of some depths in the East Sea of Korea. We just presents the distributions in February and August representing one year variation. Fig. 6 gives the horizontal variations of mean temperature at 0 m, 50 m, 100 m, and 200 m in February. From the surface up to 100 m, the temperatures show very similar patterns implying the waters are well mixed by strong winds. The mean temperatures in August (Fig. 7), however, show very big changes in their variation patterns from the surface to 100 m. The distributions in February and August give

somewhat similar patterns at 100 m and almost no noticeable differences at 200 m. This fact implies that most of seasonal variations occur from the surface to 100 m or more in the water column.

As an example of sonar operation related to seasonal variations of water mass, we try to compute sonar performance, DR, using the temperature data set depicted in Fig. 6 and Fig. 7.

We assume a target at 100 m, and the sonar ('Type B' in Fig. 5) located at 20 m (shallow) and 100 m (deep). Other parameters on the sonar and environment are same as in the previous section.

Fig. 8 shows the DR variations with the sonar depth varied between 20 m (shallow) and 100 m (deep) in February and August. For the details of performance variation, the smaller area,  $110 \text{ km} \times 260 \text{ km}$ , is selected from the larger one in Fig. 6 or Fig. 7. February and August are assumed to represent the winter and summer, respectively. When we keep the passive sonar at 20 m [Fig. 8(a), (b)], shallower depth, the DR shows very different patterns in February and August, being much poorer in August. When we change the sonar depth to be 100 m [Fig. 8(c), (d)], the DR shows very similar patterns in February and August. Moreover, the DR in February resembles the

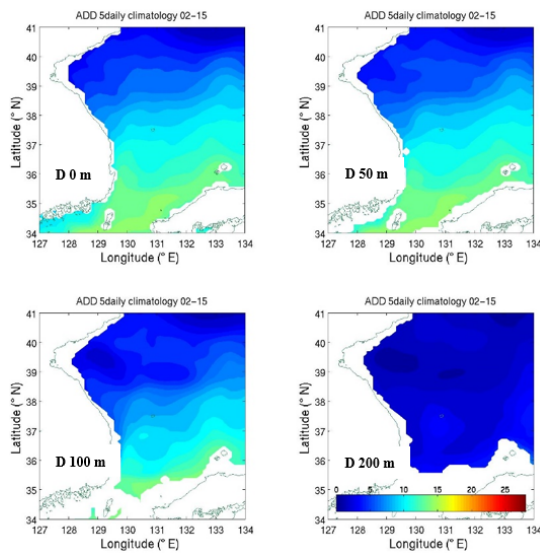


Fig. 6. Mean temperature variations at selected depths (0 m, 50 m, 100 m, and 200 m) in February.

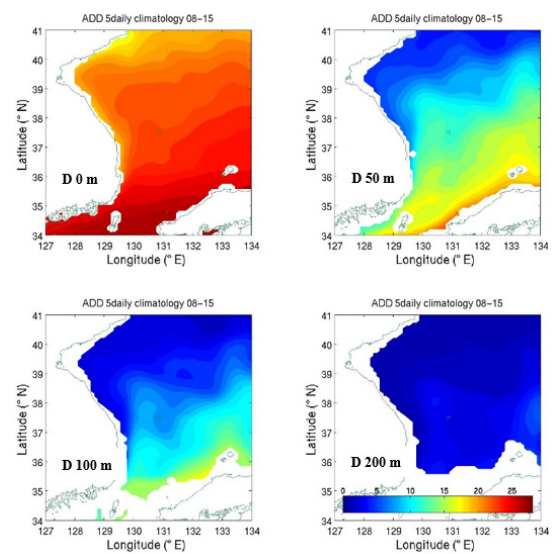


Fig. 7. Mean temperature variations at selected depths (0 m, 50 m, 100 m, and 200 m) in August.

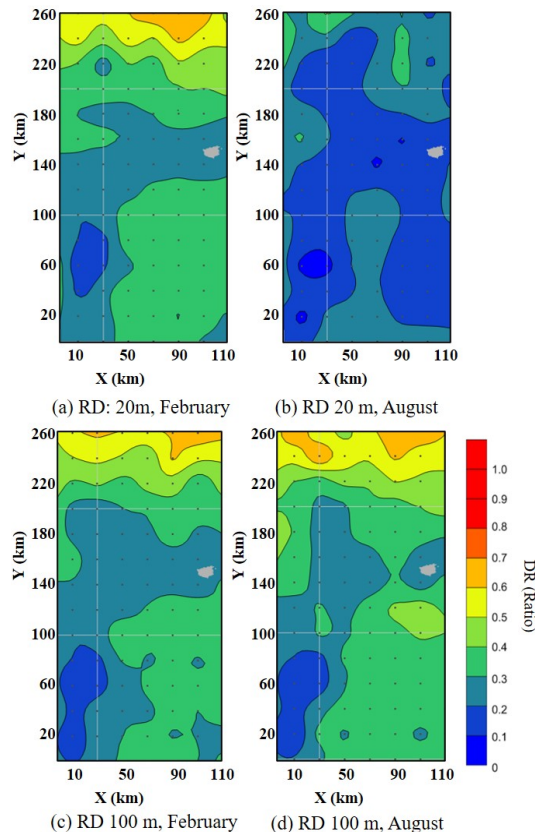


Fig. 8. Performance (DR) variations at the sonar depths 20 m (up) and 100 m (down) in February (left) and August (right).

patterns at sonar depth 20 m in February such as in the northern region. That is, we can expect very similar and good performance of little seasonal variations when we locate passive sonars to deep enough (lower than 100 m).

#### IV. Conclusions

In the coastal region of the East Sea, the spatial variations of water masses have close relations with DR and ROD, where DR and ROD show general reverse patterns of variation. The EOF analysis over temperatures shows that the 1-st mode represents typical seasonal variation and the 2-nd mode represents strength variations of surface mixed layers and currents. The two modes are estimated to explain most of the variations (about 92 %). Assuming two types of targets located at 5 m (shallow) and 100 m (deep), the passive sonar performance (DR) gives

high correlation coefficients about  $-0.9$  with mode 1 and mode 2. Most of temporal variations of temperature occur from the surface up to 200 m in the water column so that when we assume a target at 100 m, we can expect detection performance of little seasonal variations with passive sonars below 100 m.

#### Acknowledgement

This work was supported by the ROK government in 2023 under the contract No. 922012301.

#### References

1. J.-Y. Yun, L. Magaard, K. Kim, C.-W. Shin, C. Kim, and S. K. Byun, "Spatial and temporal variability of the North Korean cold water leading to the near-bottom cold water intrusion in Korea Strait," *Prog. Oceanogr.* **60**, 99-131 (2004).
2. S.-H. Lim and G.-H. Ryu, "Underwater acoustic environment and low frequency acoustic transmission in the sub-polar front region of the East Sea" (in Korean), *J. KIMST.* **12**, 415-423 (2009).
3. H.-R. Kim and J.-W. Choi, "A study on the detection performances of the integrated sonar system operated by surface vessel in the mesoscale eddy in the South-western East Sea" (in Korean), *J. KNST.* **3**, 20-45 (2020).
4. W.-K. Kim, C.-B. Cho, J.-S. Park, J. Hahn, and Y. Na, "Effects of warm eddy on long-range sound propagation in the East Sea" (in Korean), *J. Acoust. Soc. Kr.* **34**, 455-462 (2015).
5. Y. Na, S. U. Son, J. Hahn, and K. Lee, "Simulation of acoustic waves horizontal refraction using a three-dimensional parabolic equation model," *J. Acoust. Soc. Kr.* **41**, 131-142 (2022).
6. J.-H. Lee, J.-S. Kim, J.-S. Yoo, Y. H. Byun, and J.-H. Cho, "Optimal search depth for the sonar systems in a range dependant ocean environment" (in Korean), *J. Acoust. Soc. Kr.* **27**, 47-56 (2008).
7. S.-H. Yeom, S. Yoon, H. Yang and W. Seong, "Analysis of statistical characteristics of bistatic reverberation in the East Sea" (in Korean), *J. Acoust. Soc. Kr.* **41**, 435-445 (2022).
8. P. McDowell, *Environmental and statistical performance mapping model for underwater acoustic detection systems*, (Ph.D. thesis, University of New Orleans, 2010).
9. W. J. Emery and R. E. Thomson, *Data Analysis Methods in Physical Oceanography* (Pergamon press, Lexington,

- 1998), pp. 336-350.
10. M. B. Porter and H. P. Buckner, "Gaussian beam tracing for computing ocean acoustic fields," J. Acoust. Soc. Am. **82**, 1349-1359 (1987).
  11. Y.-N. Na, Y.-G. Kim, S. Kim, C. B. Cho, H.-S. Kim, Y. Lee, and S. H. Lee, "Development of submarine acoustic information management systems," J. Acoust. Soc. Kr. **24**, 46-53 (2005).

## Profile

### ▶ Young-Nam Na (나 영 남)



He graduated with a BSc in Oceanography from Seoul National University in 1985. He took the MSc degree in Oceanography from Seoul National University in 1988 and received his PhD in Underwater Acoustics at Pukyong National University, Pusan. He has been working for Agency for Defense Development since 1988. His research interest includes wave propagation in water and related simulation with environments.

### ▶ Changbong Cho (조 창 봉)



He graduated with a BSc in Oceanography from Kunsan National University in 1997. He received the Ph. D. degree in Physical Oceanography from Seoul National University in 2014. He has been working for Agency for Defense Development since 2003. His research interest includes acoustic wave propagation related to water mass.

### ▶ Su-Uk Son (손 수 옥)



He graduated with a BSc in Oceanography from Hanyang University, Ansan in 2008. He took the MSc degree in Underwater Acoustics in 2010 and received his PhD in Underwater Acoustics in 2015 and worked as Post-Doctor in 2016 at Hanyang University. He has been working for Agency for Defense Development since 2016. His research interest includes detection performance analysis related to underwater acoustics.

### ▶ Jooyoung Hahn (한 주 영)



He received BSc, MSc and PH.D degrees in earth and marine sciences from Hanyang University, Ansan, South Korea, in 1997, 2000, and 2004, respectively. Since 2005, he has been with the Agency for Defense Development, Changwon, South Korea, where he is currently a Principal Research Scientist. His research interests include channel modeling and source localization.